International Journal of Heat and Mass Transfer 116 (2018) 897–908

Contents lists available at ScienceDirect

International Journal of Heat and Mass Transfer

journal homepage: www.elsevier.com/locate/ijhmt

Experimental study on thermal flow characteristics in square serpentine heat exchangers mounted with louver-type turbulators

T.M. Liou [a,*], S.W. Chang [b], S.P. Chan [a]

[a] Department of Power Mechanical Engineering, National Tsing-Hua University, Hsinchu City 30013, Taiwan, ROC
[b] Department of System and Naval Mechatronic Engineering, National Cheng-Kung University, Tainan City 701, Taiwan, ROC

ARTICLE INFO

Article history:
Received 31 July 2017
Accepted 12 September 2017
Available online 17 October 2017

Keywords:
PIV
Infrared thermography
Louver-type turbulator
Pitch ratio
Blockage ratio
Turbulent thermal flow

ABSTRACT

The present study aims to propose innovative louver-type turbulators to enhance the heat transfer rate in three major ways, i.e. core flow disturbance, jet impingement, and extended heat transfer surface. These louvers are installed in the twin-pass square channel with a hydraulic diameter (D_H) of 45.5 mm and a fully developed inlet condition. Three parameters are examined to find out the optimal design, including the pitch ratio (Pi/D_H = 1, 2, 3, 4, and ∞), the number of slat per half louver ($1 \le N_s \le 4$), and Reynolds number ($5000 \le Re \le 20000$). Particle Image Velocimetry (PIV) and Infrared Thermometry (IT) are respectively employed to measure the detailed velocity maps and wall temperature distributions. With acquired Nusselt number (Nu) ratio, the pressure measurements are also performed to estimate the Fanning friction factor (f) and further evaluate the thermal performance factor (TPF). The results show that both $\overline{Nu}/Nu_\infty$ and $\bar{f}/f_\infty$ ratios rise with descending Pi/D_H and ascending N_s under the present test conditions. Among all the tested cases, the case with $Pi/D_H = 1$ and $N_s = 4$ provides the highest $\overline{Nu}/Nu_\infty$, almost twice the value of smooth reference; nevertheless, it suffers from high $\bar{f}/f_\infty$ penalty. It is also found that the TPF level is a relatively weak function of Pi/D_H. The new finding is that there exists a critical slat number of $N_s = 3$ above which the TPF value is a weak function of N_s. In contrast, below the critical N_s the TPF value increases with decreasing N_s. From the viewpoint of heat transfer enhancement, one could apply the louvered channel as a heat exchanger with small Pi/D_H and large N_s. The boundary layer disturbance, on the other hand, is more cost-effective than core flow disturbance as a mechanism to augment heat transfer from the viewpoint of thermal performance.

1. Introduction

Serpentine channel served as a heat exchanger has been widely applied to many engineering and industrial applications such as heating, ventilation, and air conditioning (HVAC) systems [1–3], high-pressure turbine blade [4–6], polymer electrolyte membrane fuel cells (PEMFC) [7–9], and shell-and-tube heat exchanger [10–12] to name a few. Many research groups [13–17] paid their attention to the detailed momentum and energy transport phenomena inside the smooth serpentine channel. Nevertheless, low heat transfer rates were reported as indicated by the checkerboard in Fig. 1 [15–19] and they did not meet the thermal requirements in most cases. Numerous kinds of turbulators are therefore added to the smooth heated surfaces in a periodic manner to improve the fluid mixing and elevate the heat transfer rate.

Among various types of turbulators, rib is the most frequently used one. Han and Park [20] used thermocouples and pressure taps to explore the effect of rib angle orientation (α) in rectangular channels with aspect ratios (AR) of 1, 2, and 4 for Reynolds number (Re) ranging from 10,000 to 60,000. They reported that the best heat transfer performances in the rectangular channels with α = 30-deg and 45-deg were about 30% and 5% higher than the case with α = 90-deg for aspect ratios of 1 and (2, 4), respectively. Rallabandi et al. [21] experimentally examined the effects of the rib-height to channel-height ratio and rib pitch-to-height ratio in a 45-deg ribbed square channel for $30{,}000 \le Re \le 400{,}000$. Their data demonstrated that the higher heat transfer coefficients were obtained at smaller rib pitch ratio and larger rib height ratio accompanying with higher pressure loss penalty (higher f/f_∞, Fig. 1). Mochizuki et al. [18] investigated the rib arrangements in a two-pass square channel for Re in the range of 4000–30,000. The rib pitch-to-height ratio and rib-height to channel-height ratio were 10 and 0.1, respectively, while the rib angle was varied from 30-deg to 90-deg with an interval of 15-deg. They found that the

* Corresponding author.
E-mail addresses: tmliou@pme.nthu.edu.tw (T.M. Liou), swchang@mail.ncku.edu.tw (S.W. Chang), tedchan0611@gmail.com (S.P. Chan).

https://doi.org/10.1016/j.ijheatmasstransfer.2017.09.053
0017-9310/

Nomenclature

English symbols

A	cross-sectional area (m^2)
AR	aspect ratio $= W_1/B = W_2/B$
B	channel height (m)
BR	blockage ratio
Bi	Biot number $= hD_H/k_s$
C_p	specific heat of fluid (J kg^{-1} K^{-1})
D_H	hydraulic diameter $= 4A/P$ (m)
f	fanning friction factor $= [\Delta P/(0.5\rho U_b^2)]/(4L/D_H)$
$\bar{f}$	fanning friction factor averaged over four walls
f_∞	Blasius equation for turbulent flow $= 0.079Re^{-0.25}$
h	convective heat transfer coefficient (W m^{-2} K^{-1})
h_{nc}	outer natural convection coefficient of scanned heating foil (W m^{-2} K^{-1})
k_f	thermal conductivity of fluid (W m^{-1} K^{-1})
k_s	thermal conductivity of stainless foil (W m^{-1} K^{-1})
L	channel length (m)
Δl	laser light sheet thickness (m)
Nu	local Nusselt number $= hD_H/k_f$
$\overline{Nu}$	averaged Nusselt number
Nu_∞	Nusselt number based on Dittus-Boelter correlation $= 0.023Re^{0.8}Pr^{0.4}$
N_s	numbers of slat per half louver
P	perimeter of cross-section (m)
Pi	pitch between consecutive turbulators (m)
Pr	Prandtl number $= \mu C_p/k_f$
ΔP	pressure drop across test section (Nm^{-2})
Q	volumetric flow rate (m^3/s)
q_f	convective heat flux (Wm^{-2})
q_{gen}	total heat flux generated by stainless foil (Wm^{-2})
q_{loss}	heat loss to environment (Wm^{-2})
Re	Reynolds number $= \rho U_b D_H/\mu = \rho Q D_H/A\mu$
Ro	rotation number $= \Omega D_H/U_b$
T_b	bulk fluid temperature (K)
T_w	wall temperature (K)
T_∞	ambient temperature (K)
TPF	thermal performance factor$= (\overline{Nu}/Nu_\infty)/(\bar{f}/f_\infty)^{1/3}$
Δt	Shutter of CCD camera (s)
U_b	bulk flow velocity (ms^{-1})
U	streamwise mean velocity (ms^{-1})
u'	streamwise turbulence intensity (ms^{-1})
V	transverse mean velocity (ms^{-1})
$\lvert V\rvert$	velocity magnitude across laser light sheet (ms^{-1})
W	spanwise mean velocity (ms^{-1})
W_1	width of first-pass duct (m)
W_2	width of second-pass duct (m)
W_d	divider thickness (m)
X	streamwise coordinate (m)
X*	normalized streamwise coordinate $= X/D_H$
Y	transverse coordinate (m)
Y*	normalized transverse coordinate $= Y/B$
Z	spanwise coordinate (m)
Z*, Z**	normalized spanwise coordinate, (i) X<0, $Z^{**} = Z/[(W_1 + W_2 + W_d)/2]$ (turn), (ii) X ≥ 0, Z < 0, $Z^* = [Z + (W_d/2)]/W_1$ (1^{st} pass), (iii) $X \geqslant 0, Z > 0, Z^* = [Z - (W_d/2)]/W_2$ (2^{nd} pass)

Greek symbols

α	angle of Rib (degree)
ε	emissivity of stainless steel foil
ξ	ratio of out-of-plane displacement to laser sheet thickness $= \lvert V\rvert\Delta t/\Delta l$
ρ	fluid density (kg m^{-3})
σ	Stefan-Boltzmann constant (kg s^{-3} K^{-4})
μ	fluid dynamic viscosity (kg m^{-1} s^{-1})
Ω	rotational speed of test duct (rad s^{-1})

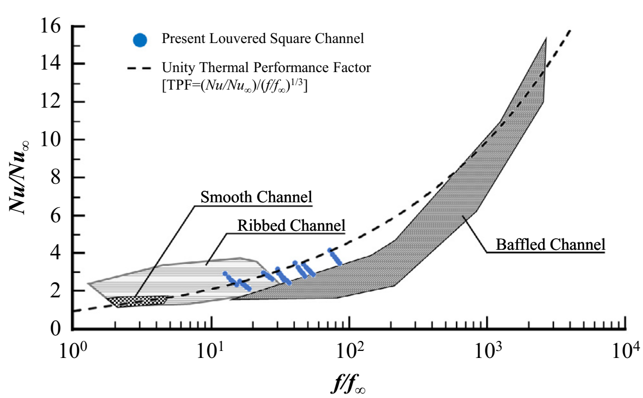

Fig. 1. Variation of Nu/Nu_∞ against f/f_∞ for the present louvered channel as well as the previous smooth channel [15–19], ribbed channel [20–24,40–44], and baffled channel [28,31].

positive rib angle for both first and second pass, denoted as (+, +), gave the maximum average Nusselt number ($\overline{Nu}$), followed by (+, −), (−, +), and (−, −), while the pressure drops in all cases had the same order.

Liou et al. [22] employed laser-Doppler velocimetry (LDV) and transient liquid crystal thermography (TLCT) to investigate 12 kinds of turbulators in a square channel at Re = 12,000. Their results showed that the direction and strength of the secondary flow with respect to the target surfaces were highly correlated to the Nusselt number (Nu) distribution. The convective mean velocity and turbulent kinetic energy were respectively the second and the third factors affecting the local heat transfer. Amro et al. [23] investigated the heat transfer performance for 45-deg and 60-deg ribs in a triangular channel with TLCT and pressure taps. The 60-deg ribs provided in general higher heat transfer enhancements than those in the 45-deg ribbed cases but suffered from the penalty of extremely high friction factors. Saha and Acharya [24] examined the effect of aspect ratio (AR = 0.25, 1, and 4) on the heat transfer and flow field in ribbed rectangular channels through solving the unsteady Reynolds averaged Navier–Stokes (URANS) equations for single Reynolds number (Re = 25,000). They concluded that the channel with higher AR had the higher heat transfer elevation because the rib-induced secondary flow consisted of multiple roll cells directed the fluid to the heated surfaces more effectively.

There was another commonly used turbulator, baffle, which had a relatively higher blockage ratio (BR) than rib (reticulation in Fig. 1). Berner et al. [25] applied LDV and flow visualization (FV) to study the flow features inside the baffled rectangular duct with AR of 5. They also presented the normalized pressure drop between two consecutive baffles on the same side. The baffle spacing and thickness normalized by channel height were respectively fixed at 0.4 and 0.05, while the BR and Re respectively varied from 0.5 to 0.9 with an interval of 0.2 and from 600 to 10,000. They found the length required to obtain periodically developed state inside the baffled channel was a function of Re and BR. Instead of heat transfer experiments, Molki and Mostoufizadeh [26]